Polymer 49 (2008) 3279–3287

Contents lists available at ScienceDirect

Polymer

journal homepage: www.elsevier.com/locate/polymer

Characterisation of polyurethane networks based on vegetable derived polyol

M. Carme Coll Ferrer [a], David Babb [b], Anthony J. Ryan [a,*]

[a] Department of Chemistry, The University of Sheffield, Brookhill, S3 7HF Sheffield, UK
[b] Polyurethanes R&D, The Dow Chemical Company, 2301 Brazosport Boulevard, B-4810 building, Freeport, Tx 77541, USA

ARTICLE INFO

Article history:
Received 19 February 2008
Received in revised form 6 May 2008
Accepted 7 May 2008
Available online 16 May 2008

Keywords:
Polyurethane networks
Vegetable polyol
Molecular weight between crosslinks

ABSTRACT

A polyurethane (PU) network based on vegetable derived polyol has been characterised and compared to a synthetic based network. Fracture mechanics studies showed the lowest tear strength for the *vegetable* networks, which decreased as molecular weight of the vegetable based polyol increased. Swelling studies were carried out to determine the molecular weight between crosslinks and polymer networks made from wholly *synthetic* polyols were shown to have higher molecular weight between crosslinks. Moreover, *vegetable* networks showed higher solubles' content. Sol-fractions were analysed by several techniques. It was found that *vegetable* networks based sol-fraction was mainly its correspondent raw polyol while low molecular weight oligomers were detected for the most part in *synthetic* networks based sol-fraction.

1. Introduction

Polyurethanes (PUs) are known for their versatility. They can be easily tailored to use in a wide range of applications [1]. However, one of the problems facing polyurethanes nowadays is their dependence on petroleum derivative products. As the oil crisis and global warming deepens, the study of PU based on renewable resources has re-emerged. PU based on vegetable oils is not new. First studies date back from the 60s [2]. Since then, a wide range of vegetable oils have been considered for the preparation of segmented PU including, safflower, sunflower, but mainly castor and soybean oils.

Vegetable oils are composed of triglycerides, i.e. a glyceride in which the glycerol is esterified with three fatty acids. The most common chain lengths in these fatty acids are 18 or 20 carbon atoms, which can be either saturated or unsaturated. When unsaturated the double bonds are located at the 9, 12 and 15 carbon. Other than in castor oil, the major unsaturated fatty acids in vegetable oils are oleic, C18:1, linoleic, C18:2, and linolenic acid, C18:3, where C18:*a* is the number of carbons C18 and the number of unsaturated bonds, *a*. Castor oil is a triglyceride of fatty acids with ricinoleic acid as the major constituent (~90%). Ricinoleic acid, *C*18:1, has an hydroxyl functional group at the 12th carbon. Its molecular weight is 933 and its hydroxyl number lies between 160 and 180. Castor oil has been mainly considered for the synthesis of semi-rigid and rigid foams [2–5]. However, for this purpose, castor oil presents two main disadvantages its low hydroxyl number and its slow rate of curing due to the presence of secondary hydroxyl [3].

Several methodologies have been successfully developed to prepare vegetable oil based polyols for general PU use. Vegetable oil has been epoxidised, followed by methanolysis to form the triglyceride polyol with a secondary hydroxyl [6]. Also, double bonds have been first converted to aldehydes through hydroformylation using either rhodium or cobalt as the catalyst. Then, the correspondent aldehydes have been hydrogenated by Raney nickel to alcohols. Primary hydroxyl based polyols are obtained with this procedure [7,8]. Ozonolysis is another method that has been reported to obtain terminal primary hydroxyl groups [9]. Low molecular weight polyols, crystalline, waxy solids at room temperature with T_g of 53 °C, 36 °C and 22 °C for model, i.e. triolein, canola and soy based PU have been reported by applying this method.

In this study, a polyether polyester polyol based on vegetable oil was employed. Polyols were obtained by transesterification of an initiator and methyl ester fatty acids [10]. The resultant polyols were primary hydroxyl with lower hydroxyl number than polyols obtained by using other methods described above. In agreement with other vegetable oils synthesized up to now, these polyols presented hydroxyl functionalities in the middle of the chain thus, when crosslinking, part of the triglycerides are left as dangling chains. Dangling chains are those chains attached at only one end. They are elastically ineffective. Therefore, possible dangling chains of different lengths in the vegetable based polyol would affect the mechanical properties when used in a network. Mark and coworkers [11–13] studied the dependence of ultimate properties on dangling chain irregularities of model poly(dimethylsiloxane). They found T_g to be generally insensitive to the concentration of dangling chains over a range 0–41.1 wt%. However, they noticed a decrease in

* Corresponding author. Tel.: +44114 222 9409; fax: +44114 222 9389.
E-mail address: tony.ryan@sheffield.ac.uk (A.J. Ryan).

0032-3861/$ – see front matter © 2008 Elsevier Ltd. All rights reserved.
doi:10.1016/j.polymer.2008.05.017

the intensity of the tan δ relaxation with increase in concentration of dangling chains over this range. Broader glass transition–good energy absorbing properties were also observed in polyurethane elastomers possessing dangling chains [14]. Furthermore, by comparison of constant values of high deformation modulus they observed that dangling chain irregularities decreased both the maximum extensibility of a network and its ultimate strength. That was further confirmed in polyurethane networks, theoretically and experimentally, by Dušek and co-workers [15].

Extensive research on the synthesis of *vegetable* polyols and characterisation of their corresponding PU has been carried out by Petrovic and co-workers [6,8,9,16–25]. In PU networks based on soybean oil with different isocyanates [21] or with polyols based on other vegetable oils but prepared also by epoxidation [17], they encountered that network properties were directly related to the crosslinking density and the structure of the isocyanate but not on the type of vegetable oil. In addition, they examined the effect of dangling chains on PU networks. To do so, they removed dangling chains of a triolein by metathesis, and they compared networks based on soy polyol with and without dangling chains. The former showed a lower T_g, which could be due to lower crosslink density, the plasticizing effect of the dangling side chains or lower content in MDI, while the later experience much lower swelling, 40% versus 95%. Furthermore, soy polyols were mixed with ethylene oxide or butane diol and MDI to prepare segmented PU by either prepolymer or one-shot method [20] with a hard segment content of 0, 10 and 40. Partial crystallinity and phase separation were found with 40% HS content with a broader distribution of domain sizes for the ethylene glycol extended system. Although the presence of hard segments lowers the crosslink density, they observed that the samples with higher HS content had higher glass transition temperatures, which could be due to the higher content of phase mixing, with higher strengths, higher moduli, lower swelling, lower elongation at break and lower impact strengths. In general, samples exhibited strong volume relaxation, which was related to dangling side chains, and loss modulus curves displayed two maxima, an α around 60 °C and a β-transition at around −60 °C. The former is associated with segmental motion, while the latter is generally attributed to the rotation of smaller groups in the main chain. Similarly β-transition was observed in soy polyol based PU crosslinked with different isocyanates [21]. PU produced from hydroformylation of soybean oil and polymeric MDI was also obtained. Their properties were strictly related to the degree of polyol conversion. The rhodium catalyzed reaction leads to a rigid plastic while the reaction catalyzed by cobalt leads to a hard rubber [8]. Recently, the performance of these soy polyols prepared either via epoxidation or hydroformylation has been compared in cast PU resins and rigid PU foams. Both systems can produce foams having the required mechanical strength. Main differences in behaviour were attributed only to differences in polyol reactivity [24]. PU prepared from triglyceride polyols by ozonolysis showed good mechanical properties and higher glass transition temperatures compared to PU from epoxidised and hydroformylated polyols of same functionality, presumably due to the absence or lower content of dangling chains in the former [9].

The aim of this work is to characterise polyurethane based networks to determine the influence of the polyol on its final mechanical properties. To do so, networks prepared on several vegetable based polyols and *synthetic* polyols have been studied.

2. Experimental

2.1. Materials

The present study makes use of several samples which were prepared at the Dow Chemical company at Midland, Michigan. The

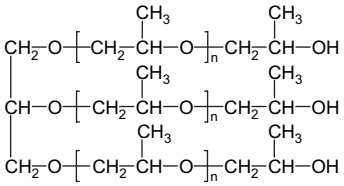

Fig. 1. Chemical structure of the VOR, VORA and VORB polyols.

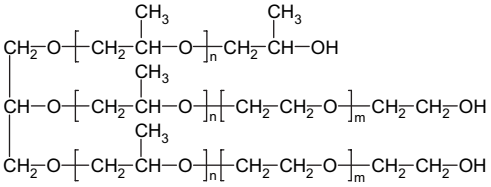

Fig. 2. Estimation of the chemical structure of the POH polyol.

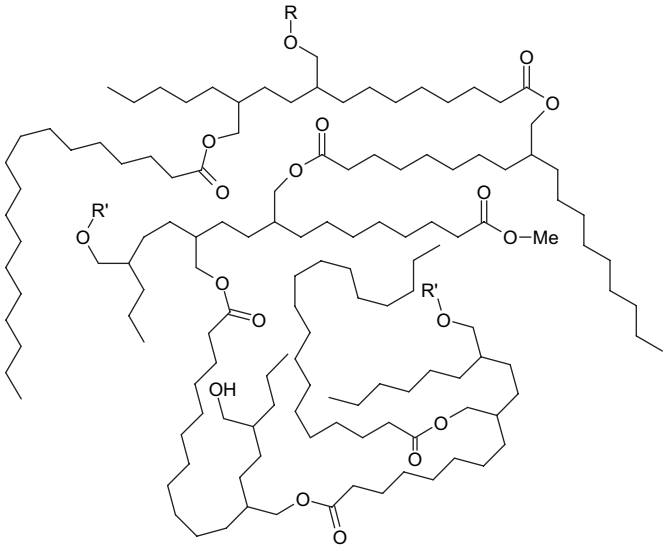

Fig. 3. Possible chemical structure of the *vegetable* polyols estimated by ^{1}H NMR, where *R* is the initiator and *R′* is randomly transesterified fatty acids.

isocyanate used, TDI, was an 80:20 mixture of 2,4-and 2,6-toluene diisocyanate isomers. Several polyols, synthetic based, *synthetic*, and vegetable based, *vegetable*, were investigated. The former are designated as VOR, VORA, VORB and POH while the latter are designated as NOP, REFA and REFB. VOR, VORA and VORB are commercial oxypropylated derivative of glycerol. POH is an oxypropylated derivative of glycerol, with at least a 78% ethylene oxide cap. Vegetable based polyols are experimentally mixed polyether polyester polyol, based on fatty acids esterified together. A representative chemical structure for each type of polyol, *synthetic* VOR, *synthetic* POH and *vegetable* polyol is shown in Figs. 1–3, respectively. Their molecular weight and OH number are summarized in Table 1. Dabco T-9 (Air

Table 1
Molecular weight and hydroxyl number of the polyols used in this study

Polyols	M_w/g mol^{-1}	OH number
NOP	2690	83
REFA	5400	35
REFB	1700	98
POH	7200	31
VOR	3000	56
VORA	3500	48
VORB	2100	79

Products) was used as a gelling catalyst to ensure the quantitative yield of the urethane.

Elastomer formulation was based on 100 parts of polyol. An isocyanate index of 100 pphp and 0.5 pphp (parts per hundred polyol) Dabco T-9 was maintained throughout the work. A one-shot, hand-cast technique was used to form polyurethane networks at room temperature. First, the polyol was dried and degassed. Then, polyol and catalyst were weighed in a 250 ml beaker and pre-weighted TDI was added slowly by syringe. The mixture was stirred with Heidolph mechanical mixer equipped with a triple blade at 400 rpm, until it became clear. The reaction mixture was then poured quickly into a mould and cured overnight at room temperature.

2.2. Characterisation techniques

2.2.1. Extractions

Extractions were performed in a soxhlet apparatus with approximately 200 ml of toluene for 24 h. The samples were weighed before and after the extraction, allowing the extracted sample to dry in a fume hood until constant weight. The soluble fraction was also dried. The weight loss was calculated from the weights of the dry samples before and after the extraction. Results are an average of four measurements, corresponding to two different elastomer samples.

2.2.2. Fourier transform infrared (FT-IR)

FT-IR spectra were recorded on a Perkin Elmer infrared spectrophotometer (Spectrum RX I FT-IR system), employing a DuraSample IR IITM Single Reflection Diamond Attenuated total reflection (ATR) accessory. The spectra were obtained at a resolution of 4 cm^{-1} and employing 64 scans. No sample preparation was required.

2.2.3. Gel permeation chromatography (GPC)

GPC with a column set comprised of one Phenogel 5 μm 5 cm × 0.78 cm pre-column (Phenomenex), two Phenogels 5 μm 30 cm × 0.78 cm mixed bed columns (Phenomenex), one Phenogel 5 μm 30 cm × 0.78 cm 5×10^4 Å single porosity column (Phenomenex) and one Phenogel 5 μm 5 cm × 0.78 cm 5×10^3 Å single porosity column (Phenomenex). A mixture of tetrahydrofuran (THF) and dimethylamine (DMA) (90:10, v/v) was used as a carrier solvent, and monodisperse polystyrene standards were used for instrument calibration. The column temperature was maintained at 30 °C and the flow rate was 1 ml min^{-1}. Sample solutions (0.2 wt%) in THF/DMA (90:10, v/v) were filtered and injected into the system. Data obtained from the detector were analysed by Polymer Laboratories "Caliber" software.

2.2.4. Thermal analysis

Thermal analysis measurements were carried out in a Perkin Elmer Pyris 1 differential scanning calorimetry (DSC). Samples, 10–15 mg, were encapsulated in aluminium pans and annealed at 120 °C for 2 min to drive off possible absorbed moisture. Then, they were scanned from −100 °C to 80 °C at a heating rate of 10 °C/min under nitrogen atmosphere. The glass transition temperature, T_g, was taken at the midpoint of the transition in heat capacity. Four scans per each sample were averaged.

2.2.5. Density

Density was calculated by means of Archimedes' principle (buoyancy method). The density of the networks is an average of four measurements, corresponding to two different elastomer samples.

2.2.6. DMTA

DMTA measurements were conducted using a Rheometrics RSA II solids analyser. The samples were tested in compression mode to obtain dynamic flexural modulus and mechanical damping as a function of temperature. A frequency of 1 Hz and a strain of 1% were employed for all the samples. Rectangular specimens of 15 × 5 × 5 mm were cut with a razor blade. Samples were cooled from ambient to −60 °C and then held at this temperature for 5 min. The samples were then heated at a rate of 5 °C min^{-1} to 120 °C.

2.2.7. Swelling

Swelling measurements were performed on rectangular pieces weighting approximately 1 g. Specimens were placed in test tubes containing 20 ml of solvent and allowed to swell at room temperature to reach equilibrium. Periodically, the samples were removed from the solvent, blotted dry on a paper towel, and then weighed quickly and accurately until constant weight. Data from at least four different samples of each network were averaged.

2.2.8. Fracture

Fracture measurements were carried out on a Housfield model H10KT. The specimens measured were approximately 25 × 3 mm with notches of various depths, from 1.5 mm to 15 mm. A standard test piece of the elastomers used is shown in Fig. 4. Tests were performed at room temperature. Forces employed were of the order of tens *N*. Results are an average of at least 25 specimens.

2.2.9. SEM

SEM micrographs were taken on a Camscan SEM operating at an accelerating voltage of 10 kV. Rectangular pieces of approximately 2.5 × 1 mm where cut with a razor blade from the crack. Samples were exposed overnight in a vacuum oven under the conditions of room temperature and 100 mmHg. Then, these were mounted on aluminium stub using double-coated cellulose tape and coated with gold by an EMSCOPE SC500 sputter coater for 4 min.

3. Analysis of the results

3.1. Crosslink density

The Flory–Renher equation for equilibrium swollen networks was used to calculate the average molecular weight of chain between crosslinks, M_c [26]

$$M_c = \frac{V_1 \rho_2 \left(V_{2m}^{1/3} - \frac{V_{2m}}{2}\right)}{-\left[\ln\left(1 - V_{2m}\right) + V_{2m} + \chi V_{2m}^2\right)\right]} \quad (1)$$

where ρ_2 is the initial density of the polymer, V_1 and V_{2m} are the molar volume of the solvent and the volume fraction of polymer in the swollen network and χ is the polymer–solvent interaction parameter, which can be estimated by [27],

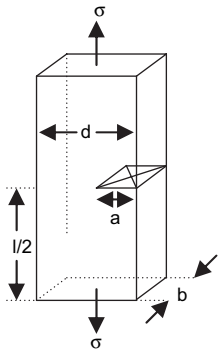

Fig. 4. Standard single-edge notched specimen used.

$$\chi = 0.34 + \frac{V_1}{RT}(\delta_2 - \delta_1)^2 \quad (2)$$

where δ is the solubility parameter. By convention, the components 1 and 2 are the solvent and the polymer, respectively.

The solubility parameter of each crosslinked polymer was determined by swelling experiment. Networks were swollen to equilibrium in several solvents of varying solubility parameter. Then, the swelling coefficient, Q, was plotted against the various solvents' solubility parameter. The solubility parameter at the maximum swelling coefficient was assigned to the polymer solubility parameter. The swelling coefficient, Q, is defined by

$$Q = \frac{m - m_0}{m_0} \times \frac{1}{\rho_s} \quad (3)$$

where m is the weight of the swollen sample, m_0 is the dry weight, and ρ_s is the density of the swelling agent.

3.2. Energy for tearing

The energy of fracture of elastomers, G_c, was determined with tear strength experiments. The data were analysed using fracture mechanics based on an extension of Griffith's hypothesis [28,29] and assuming that the energy dissipation around the crack-tip occurs in a manner independent of the test piece geometry [29]. Mathematical derivations are reported elsewhere. Thus, for a single-edge notch (SEN) specimen, the energy for tearing of elastomers, G_c, is [28]

$$G_c = 2kaW_0 \quad (4)$$

where k is a strain dependent constant, a is the notch depth, and W is the remote strain energy density in the sample (i.e. away from the crack) and may be taken as the integral of the stress–strain curve. The approximate theoretical relation for k, proposed by Lake [30] and further confirmed by Ryan [28], was used,

$$k = \frac{\pi}{\lambda^{1/2}} \quad (5)$$

where λ_c is the extension ratio of the specimen at the onset of crack propagation.

4. Results and discussion

The weight loss results of the networks studied together with the raw polyol equivalent weight, EW, is shown in Table 2. The weight loss is an indication of the number of chains that are not attached to the system. It is expected to increase with the equivalent weight, of the polyol. As observed in Table 2, *vegetable* polyol, i.e. NOP, REFA, REFB, showed the highest weight loss percentage. Comparing by groups, *synthetic* networks, i.e. POH, VOR, VORA and VORB, versus *vegetable* networks, the latter showed over double the weight loss of the former per similar polyol equivalent weight. However, it is of note that within the *synthetic* networks and within *vegetable* networks, the amount of weight loss increased with equivalent weight as expected.

Table 2
Polyol equivalent weight, EW, and soluble fraction of the polyurethanes studied

Systems	EW/g eq^{-1}	Sol-fraction/%
NOP	680	6.2 ± 0.2
REFA	1625	14.6 ± 0.4
REFB	570	6.4 ± 0.2
POH	1810	6.4 ± 0.3
VOR	1000	3.2 ± 0.3
VORA	1170	5.0 ± 0.4
VORB	715	2.5 ± 0.2

The gel fraction was dried and further analysed by DSC. T_g of the networks before and after extraction is shown in Table 3. Good agreement was encountered between the T_g of the as-formed network and that of the extracted network.

In addition, the solubles' fraction was dried and analysed by FT-IR. Spectra of NOP and VOR sol-fractions are shown in Figs. 5 and 6. The former as a representative for *vegetable* networks and the latter for *synthetic* networks, since similar trends to these were

Table 3
Polyol equivalent weight, EW, and T_g of the networks, T_gn, gel fraction, $T_g$gf, raw polyol, T_gp, and sol-fraction, T_gs for the systems studied

Systems	EW/g eq^{-1}	T_gn/°C	$T_g$gf/°C	T_gp/°C	T_gs/°C
NOP	680	−42 ± 2	−41 ± 3	−61 ± 2	−59 ± 1
REFA	1625	−46 ± 3	−49 ± 1	−60 ± 2	−57 ± 2
REFB	570	−40 ± 1	−37 ± 3	−62 ± 1	−57 ± 1
POH	1810	−60 ± 2	−61 ± 1	−68 ± 1	−65 ± 1
VOR	1000	−53 ± 4	−52 ± 1	−68 ± 1	−57 ± 2
VORA	1170	−57 ± 1	−57 ± 1	−69 ± 1	−65 ± 1
VORB	715	−44 ± 1	−45 ± 1	−66 ± 1	−57 ± 2

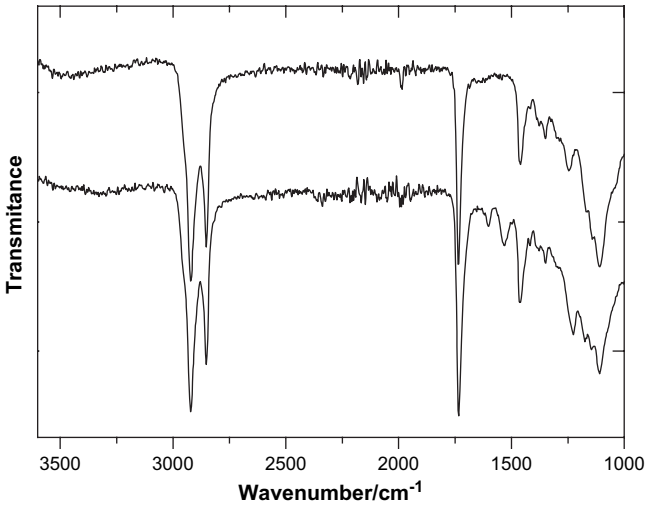

Fig. 5. IR spectra of dried NOP polyol (top spectrum) and dried NOP sol-fraction (bottom spectrum).

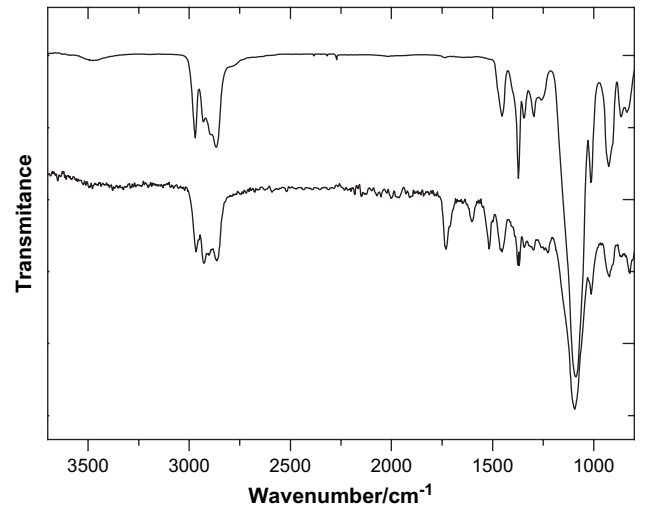

Fig. 6. IR spectra of dried VOR polyol (top spectrum) and dried sol-fraction VOR (bottom spectrum).

encountered in the other polyols. Spectra of the correspondent dried polyol have been included in Figs. 5 and 6 for comparison. Surprisingly, the spectrum of the sol-fraction for *vegetable* networks showed the resonance of its corresponding dried polyol. No sign of low molecular crosslink molecules with urethane bonds was detected. However, *vegetable* polyols are ester based which make difficult the detection of low molecular weight oligomers due to the superposition of bands. In contrast to *vegetable* networks, spectra for *synthetic* networks reflected the presence of free urethane and urea. Thus, in order to further confirm these results, T_g of all the sol-fractions was measured and compared to the T_g of its corresponding dried polyol. Results are summarized in Table 3. In general, the gap between raw polyol T_g and sol-fraction T_g values was found to be larger in *synthetic* polyols. Higher T_g value in sol-fraction than in raw polyol is the indicative of high M_w or H-bonded components, which in this case would be attributed to oligomers. Comparing *vegetable* networks between them, only REFB, the network based on the lowest polyol equivalent weight, showed slightly higher sol-fraction T_g compared to that of the polyol. In the other two *vegetable* networks, NOP and REFA no apparent gap between T_g was observed. It is also observed that the highest equivalent weight polyols, either *synthetic*, POH and VORA, or *vegetable*, REFA, showed sol-fraction T_g very similar to their corresponding dried polyol T_g.

Furthermore, the sol-fractions were analysed by GPC to gain some information about their chemical composition. Similar chromatograms were observed within *vegetable* networks and within *synthetic* networks. Therefore, only a representative of each type is shown. The former is shown in Fig. 7 while the latter is shown in Fig. 8, Since it is known that the *vegetable* polyols were synthesized from an initiator and methyl ester fatty acids, other than the chromatogram for NOP polyol, the chromatograms for the initiator and hexyl methyl stearate (HMS) were also added for comparison. As expected from DSC and FT-IR results, *vegetable* polyols were found to be the main contributor of the sol-fraction and only a small peak at higher retention time was observed which is due to slightly higher molecular weight oligomers than the polyol. The peak observed at 17 min was attributed to the antioxidant package while the peak around 20 min corresponded to the marker. In the case of *synthetic* polyols, peaks of higher molecular weight than the polyol itself were observed. Contrary to the sol-fraction of *vegetable* networks, the presence of polyol in the sol-fraction is less important. That the polyurethane forming reaction ran to completion for each type of polyol was confirmed by

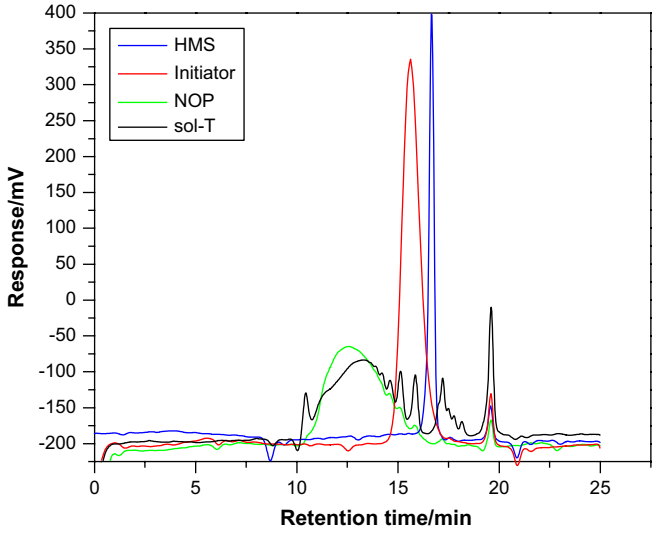

Fig. 7. Gel permeation chromatograms for NOP polyol, HMS, initiator and NOP solubles (sol-T).

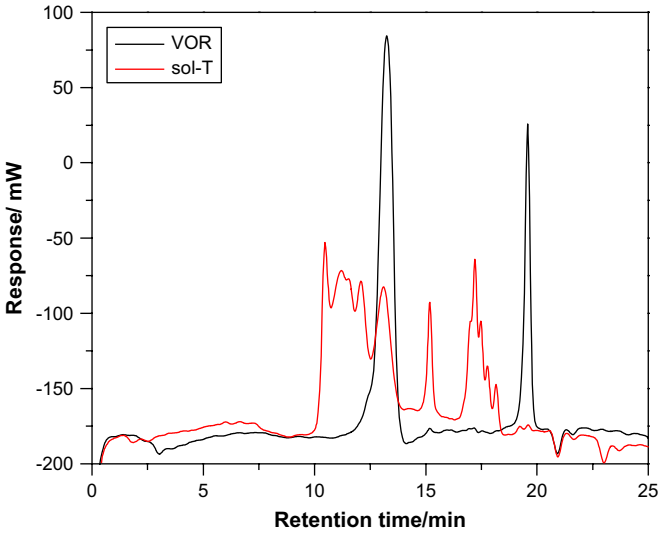

Fig. 8. Gel permeation chromatograms for VOR polyol and VOR solubles (sol-T).

a combination of techniques (IR, DSC and GPC). IR spectra and DSC curves of the polyol, solubles and network, and GPC chromatogram of the solubles were taken in consideration, there was no residual isocyanate present and further reaction could not be induced at high temperatures.

The extraction experiments showed clearly that there is a considerable gel fraction and the mechanical properties will be dominated by the crosslink density, which is the number of elastically active chain segments per unit of volume. The crosslink density was calculated following Flory–Rehner theory based on an affine network, see Eq. (1). It involves previous determination of the polymer–solvent interaction parameter and solubility parameter of the network; see Eqs. (2) and (3), respectively.

The solvents used to determine the swelling coefficient with their correspondent solubility parameter and hydrogen-bonding tendency are shown in Table 4. Chloroform and dichloromethane were the solvents that swelled the networks the most. Swelling coefficient values together with their correspondent Gaussian fits obtained for each network are shown in Fig. 9. The maximum on each curve is used as its solubility parameter, ∂p. Further calculations led to an estimation of χ and M_c. Toluene was the solvent chosen for all the networks in these calculations. The χ and M_c results for each network, as well as those estimated for ideal reference, are shown in Table 5 and graphically shown in Fig. 10. As expected the M_c is directly related to the EW in all the networks. Two markedly trends were observed. *Vegetable* networks showed better approach to an ideal network while *synthetic* networks showed the highest M_c. At the view of these results, it is vital to understand the theory involved behind them. A brief review is discussed below.

The values of M_c were obtained by using Flory–Rehner equation, which is based on an affine model network. In an affine network the crosslinks are fixed and consequently their positions deform

Table 4
Solubility parameter and H-bonding group of the solvents studied

Solvents	$\delta/(\text{cal/cm}^3)^{1/2}$	H-bonding group[a]
THF	9.1	M
p-Xylene	8.8	M
Triethylamine	7.4	S
1,4-Dioxane	10	M
1-Butanol	11.4	S
Chloroform	9.3	P
Toluene	8.9	P
Dichloromethane	9.7	M

[a] Being poorly, moderately and strongly hydrogen bonded.

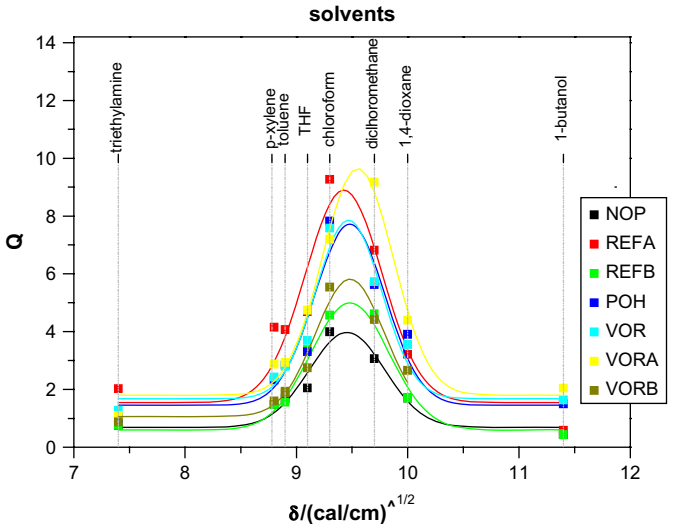

Fig. 9. Gaussian fit of the swelling coefficients versus solubility parameter for the networks studied.

Table 5
Molecular weight between crosslinks of the networks studied

Networks	EW/g eq^{-1}	X	M_c/g mol^{-1}	Ideal M_c/g mol^{-1}
NOP	680	0.336447	1374 ± 116	1534
REF A	1625	0.335714	4337 ± 250	3424
REF B	570	0.33801	1433 ± 87	1314
VOR	1000	0.336447	3568 ± 264	2174
VORA	1170	0.335418	5025 ± 251	2514
VORB	715	0.331275	1574 ± 78	1604

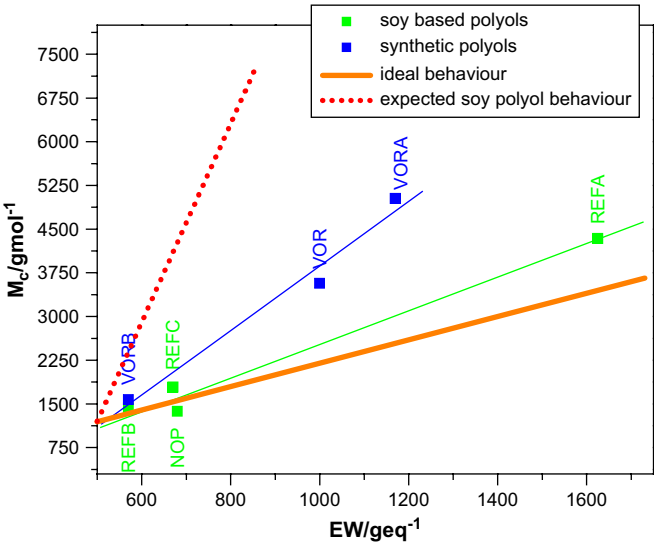

Fig. 10. Plot of molecular weight between crosslinks (M_c) versus polyol equivalent weight for the systems studied, an ideal system and *vegetable* expected system.

affinely with macroscopic strain. The chains between the crosslinks are, however, free to take any of the great many possible conformations. The affine network model also assumes that chain segments are represented by Gaussian statistics, the entropy of the network is the sum of the entropy of the individual chains, all different conformational states have the same energy and that the network is isotropic at rest state and incompressible during deformation. Therefore, it is important to emphasize the points that are not directly addressed by this statistical theory. Between them are loose chain ends, dangling chains, temporary and permanent chain entanglements and intramolecular crosslinks. Thus, any deviation from the ideal molecular weight would be attributed to the latter points. Comparing *vegetable* and *synthetic* polyols' chemical structure, it would be expected to obtain fewer irregularities in *synthetic* networks. If so, then, swelling would be expected higher in *vegetable* networks. In addition, it is important to emphasize the higher content of sol-fraction encountered in *vegetable* networks. The presence of sol-fraction is expected to further help the swelling on a network. It is known that linear molecules act as a good solvent for the network crosslinking points (clusters). Therefore, these clusters would extend, resulting in increased swelling [31,32]. Thus, considering these two points, irregular chemical structure with dangling side chains and higher sol-fraction content, the swelling in *vegetable* networks would be expected to be much higher than that in *synthetic* networks. This expected trend has been included in Fig. 10. However, as hasalready mentioned above and can be observed in Fig. 10, experimental results are drastically lower. The M_c values for *vegetable* networks were measured to be even lower to those for *synthetic* networks, at any polyol EW. The reason for these lower M_c values for *vegetable* networks points back to the composition of the sol-fraction encountered, mainly raw polyol, and to their irregular chemical structure. In relation to the latter, other than dangling side chains, loops and entanglements in *vegetable* polyols that could improve swelling; it is of note that the reactive centres in *vegetable* based polyols, OHs, are in the middle of the chain. As a consequence that could result in the formation of networks with a large distribution of molecular weights between crosslinks. Considering that the hydroxyls in the *vegetable* polyol used could be located in C9, C12 and C15 from the ester, the possibility of distinct M_c values exists. For instance, M_c could be as low as 54 g mol^{-1}, if two hydroxyls in the same chain were reacted to isocyanate or 262 g mol^{-1}, if two hydroxyls from two fatty acids at C9 were reacted to isocyanate. These possibilities are represented in Fig. 11. The M_c possibilities are *endless*, which would result in a multimodal network with similar M_c values. Mainly bimodal but also trimodal networks have been extensively studied [33,34]. Bimodal networks are known to enhance the mechanical properties when synthesized by end-linking short and long chains whose molecular weights differ by a factor of 10 or more [33]. In the case of trimodal networks, it has been observed that the ultimate properties are only enhanced when the third chain type incorporated to a bimodal network of long and short chains is very long. That is because the very long chain increases the extensibility of the network and a large amount of additional energy may be stored in the system until the very long chains reach their fully extended lengths [34]. Thus, back to the *vegetable* networks used in this study, the presence of a multimodal network with no drastically enough different M_c, would explain the low swelling observed, and therefore, the low resultant M_c obtained compared to *synthetic* networks.

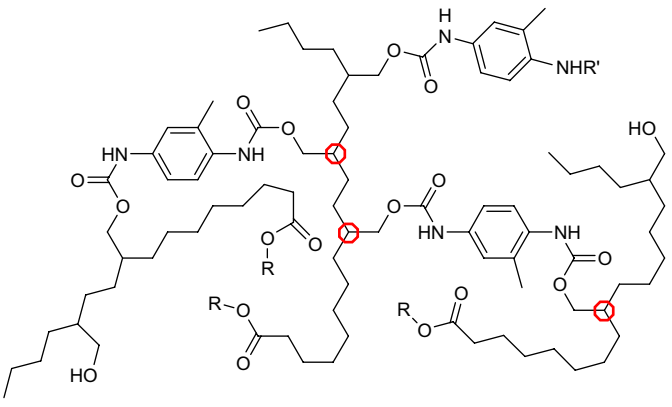

Fig. 11. Estimation of two possible low M_c in *vegetable* networks.

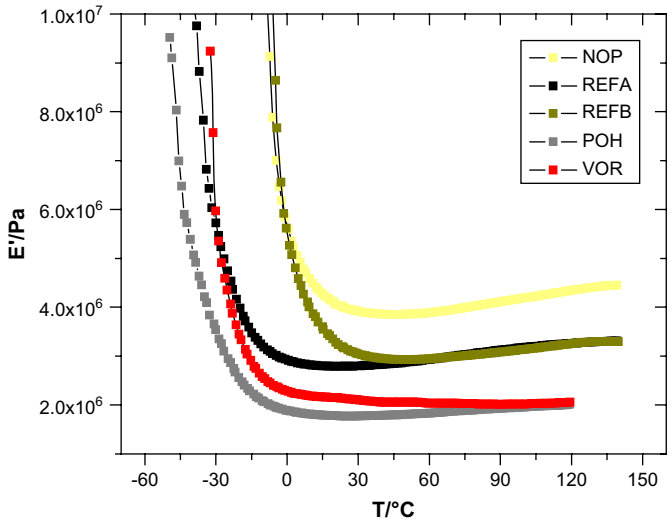

Fig. 12. Plot of elastic modulus, (E') versus temperature for the systems studied.

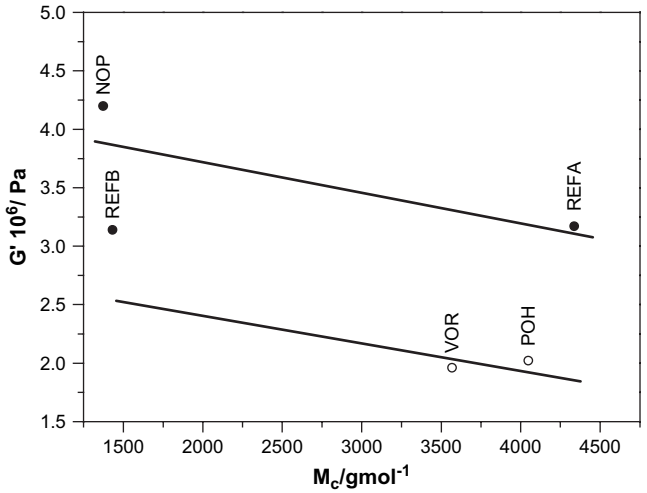

Fig. 14. Plot of elastic modulus, (G') versus the molecular weight between crosslinks for *vegetable* systems (closed symbols) and *synthetic* systems (open symbols) studied.

The temperature dependence of the storage modulus, E', and the mechanical damping, tan $\delta = E''/E'$, are shown in Figs. 12 and 13, respectively. Due to difficulties encountered on clamping specimens at low temperatures, it was not possible to obtain α-transition for the highest molecular weight polyol networks, POH and REFA in the tan δ curves. The transition from the glassy state to the rubbery state in the storage modulus curves could not be revealed either. Thus, even with limited DMTA data, some information could be extracted. The highest values of stiffness, i.e. modulus in the region of the rubbery plateau is higher, were observed for *vegetable* networks. It is known that the stiffness of an elastomer decreases with M_c, i.e. $G = \rho RT/M_c$, so a master curve is anticipated in a plot of G versus M_c. Therefore, in order to visualize this relationship, a representative plot of the modulus at 100 °C versus M_c determined by swelling is shown in Fig. 14. The expected decrease in stiffness as the M_c increases can be seen but the peculiar behaviour of *vegetable* networks that with similar M_c showed higher stiffness than *synthetic* networks is clearly observed. Results that would further agree with the case of a multimodal *vegetable* network, which would limit the extensibility of the network.

The glass temperature, taken as the temperature corresponding to a maximum in tan δ, was observed to be different from the T_g value measured by DSC. While a slightly lower value is encountered for VOR network, for *vegetable* networks, NOP and REFC, 30 °C differences was encountered. The difference is a result of the intrinsic differences in the techniques. DMTA measurements are transitional peaks. DSC is a non-mechanical measurement and transitional behaviour is determined from the onset temperatures [35].

Previous studies on poly(dimethylsiloxane) showed that T_g was found to be independent of the crosslink density [11,12] in contrast to the linear decrease in T_g with $1/M_c$ reported for model networks of polyglycols [36]. In the systems studied, it was found that in general T_g, values determined by DSC, followed the latter trend, with amplitude depending on the polyol composition. This M_w dependence of T_g is described by the Flory–Fox equation, which follows a free volume approach, assuming that the free ends contribute to an excess of free volume [37]. Results are represented in Fig. 15. From the plot, it is noted that in general *synthetic* networks are more flexible than *vegetable* networks, i.e. *synthetic* networks showed lower T_g. It is important to emphasize that higher T_g in segmented PU based on a type of soy oil polyol when compared to the segmented PU based on the former polyol but without dangling side chains have been reported in the literature [16]. It is also observed that the decrease in T_g with $1/M_w$ is less spectacular in

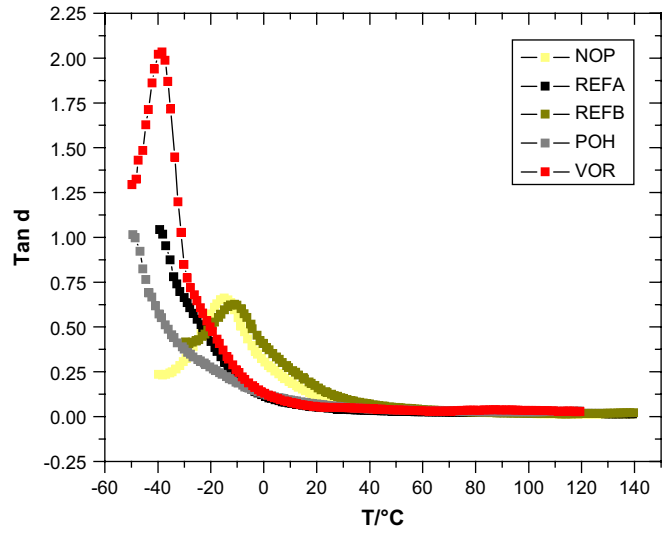

Fig. 13. Plot of tan δ for the systems studied.

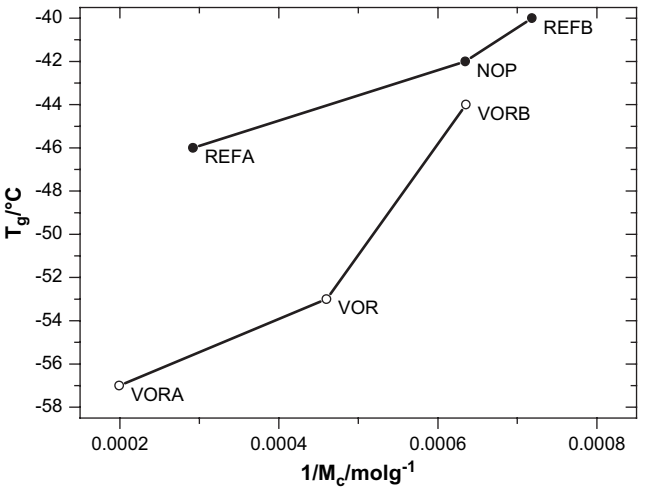

Fig. 15. Plot of dependence of T_g on the M_c for *vegetable* networks (closed symbols) and *synthetic* networks (open symbols) studied.

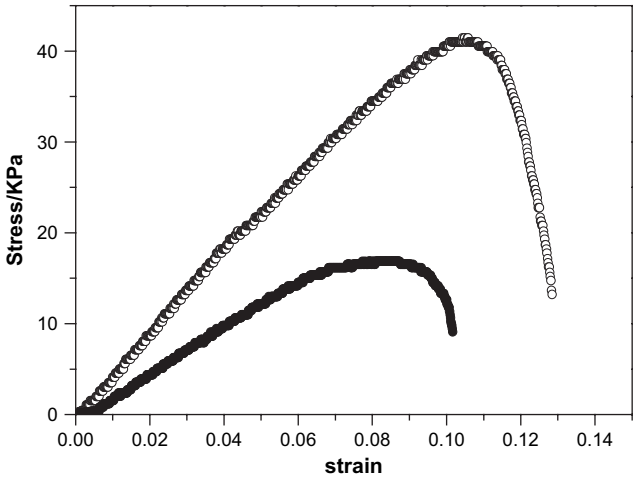

Fig. 16. Stress–strain curves for REFA notch specimens containing notch depths of 4.42 mm (open symbols) and 15.54 mm (closed symbol).

vegetable polyols. The presence of dangling side chains, i.e. chains elastically ineffective, and lower and broad distribution of M_c could explain this behaviour.

Measurements of tear strength were carried out on the networks. It was found that in general the tensile properties reduced by the notch increase, as illustrated in Fig. 16. The energy needed to propagate the crack, W_c, was obtained by integrating the area under the stress–strain curve for each specimen. Then, from the slope of the plots of $2kW_0$ versus $1/a$, values of critical strain energy release rate or energy for tearing, G_c were obtained. The plots in all cases were linear and passed through the origin, which is in good agreement with the prediction of fracture by tearing. A typical example of such a plot is given in Fig. 17 which was calculated with approximately 35 specimens. The results corresponding to all the networks are summarized in Table 6. *Vegetable* networks not only showed the lowest G_c but also showed a linear decrease in energy for tearing with the increase of molecular weight and M_c. Conversely, VOR based network, showed much higher energy for tearing even though the M_c was much bigger. The dependence of energy for tearing on M_c is represented graphically in Fig. 18. These results agree with previous ones, i.e. a toughness increase has been observed from DMTA curves, which means limited extensibility, and as a consequence, it breaks easily, thus, the lower energy required for tearing measured.

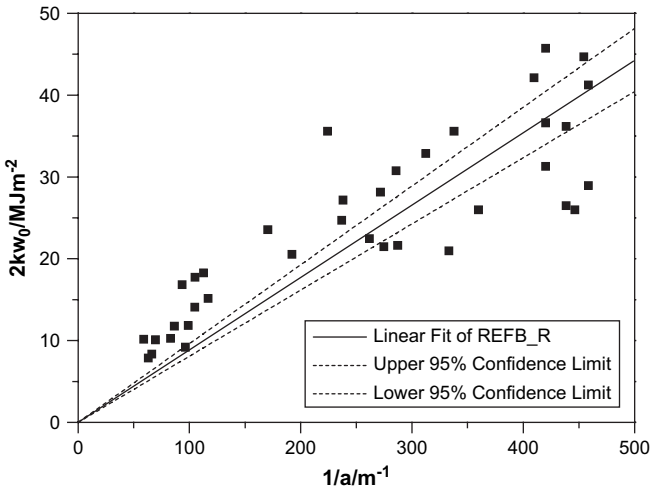

Fig. 17. A typical tear strength plot of $2kW_0$ versus $1/a$ for REFB.

Table 6
Energy for tearing of the networks studied

Product	M_w/g mol^{-1}	G_c/kJ m^{-3}
NOP	2690	84 ± 5
REFA	5400	69 ± 3
REFB	1700	88 ± 4
VOR	3000	150 ± 7
POH	7200	127 ± 6

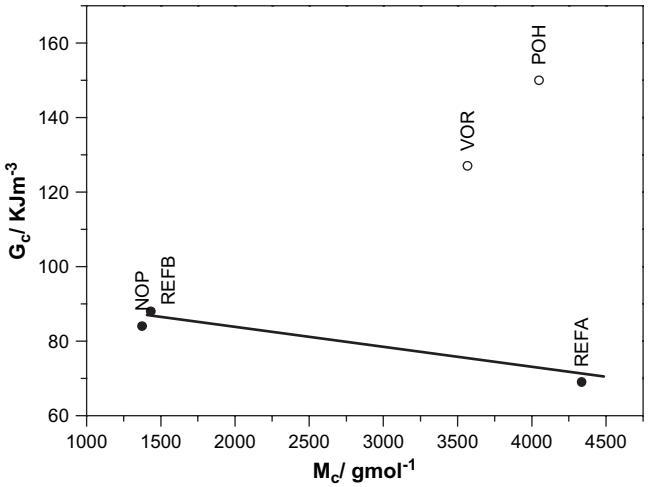

Fig. 18. Plot of dependence of the energy for tearing with molecular weight between crosslinks from swelling experiments for *vegetable* networks (closed symbols) and *synthetic* networks (open symbol).

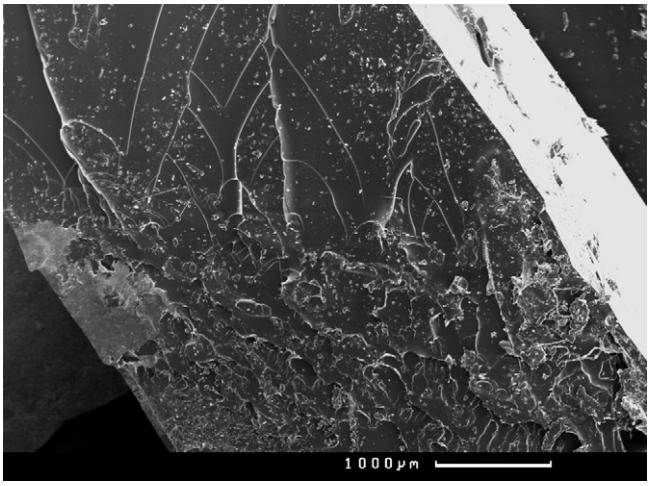

Fig. 19. SEM of a surface fracture for a NOP network.

The elastomers' fracture was investigated by SEM. All networks, *synthetic* and *vegetable*, showed a brittle fracture, which was expected due to their low molecular weight. A representative SEM of the surface fracture is shown in Fig. 19.

5. Conclusions

Vegetable networks investigated showed the highest percentage of weight loss, which was mainly, attributed to its correspondent polyol by GPC, DSC and IR measurements. In contrast, *synthetic* networks showed lower weight loss which contained basically low molecular weight oligomers.

The determination of molecular weight between crosslinks using the Flory–Rehner equation based on an affine network model,

led to higher values than those estimated for an ideal network. That was attributed to network irregularities not considered by the model. A linear dependence of the molecular weight between the crosslinks with equivalent weight of the polyol was observed. Lower M_c values were observed for *vegetable* networks which are in contrast to the large sol-fraction. In an homogeneous network a high sol-fraction is normally associated with a larger M_c and the possibility of a multimodal network with similar M_c was suggested for *vegetable* networks to explain this low swelling, and thus, low M_c measured.

The only relaxation observable by DMTA was the glass transition and other relaxations, such as those associated with dangling chains, were not observed. In general, T_g was found to decrease with polyol depending rate. Furthermore, higher modulus, i.e. limited extensibility, was encountered for *vegetable* networks. Results that would further agree with the behaviour of a multimodal network.

Although all samples showed brittle fracture, a higher energy for tearing was experienced for *synthetic* networks, being almost double of that necessary for tearing *vegetable* networks. In addition to that, the energy for tearing in *vegetable* networks was encountered to decrease as equivalent weight and M_c increased, contrary to any reasonable expectation.

Acknowledgments

We would like to thank The Dow Chemical Company for suggesting this research topic and providing the necessary financial support.

References

[1] Woods GW. The ICI polyurethanes book. The Netherlands: J. Willey & Sons; 1987.
[2] Pande CD, Kapoor SK, Bajaj I, Venkataramani B. Indian Journal of Technology 1966;4(4):109–13.
[3] Baser SA, Khakhar DV. Cellular Polymers 1993;12(5):390–401.
[4] Pande CD, Venkataramani B. Indian Journal of Technology 1968;6(10):310–1.
[5] Venkataramani B, Pande CD. Indian Journal of Technology 1969;7(9):289–92.
[6] Guo A, Javni I, Petrovic ZS. Preparation and characterization of soy-based polyols. Abstracts of Papers, 227th ACS National Meeting, Anaheim, CA, United States; March 28–April 1 2004.
[7] Lyon CK, Garrett VH, Frankel EN. Journal of the American Oil Chemists' Society 1974;51(8):331–4.
[8] Guo A, Demydov D, Zhang W, Petrovic ZS. Journal of Polymers and the Environment 2002;10(1/2):49–52.
[9] Petrovic ZS, Zhang W, Javni I. Biomacromolecules 2005;6(2):713–9.
[10] Gruenbauer HJ. In: Dow Benelux BV, editor. The Dow Chemical Company; 2004.
[11] Andrady AL, Llorente MA, Sharaf MA, Rahalkar RR, Mark JE, Sullivan JL, et al. Journal of Applied Polymer Science 1981;26(6):1829–36.
[12] Andrady AL, Llorente MA, Mark JE. Polymer Bulletin (Berlin, Germany) 1992; 28(1):103–8.
[13] Jiang CY, Mark JE. Polymer Preprints (American Chemical Society, Division of Polymer Chemistry) 1983;24(2):92–3.
[14] Lee YL, Sung PH, Liu HT, Chou LC, Ku WH. Journal of Applied Polymer Science 1993;49(6):1013–8.
[15] Dusek K, Duskova-Smrckova M, Fedderly JJ, Lee GF, Lee JD, Hartmann B. Macromolecular Chemistry and Physics 2002;203(13):1936–48.
[16] Zlatanic A, Petrovic ZS, Dusek K. Biomacromolecules 2002;3(5):1048–56.
[17] Zlatanic A, Lava C, Zhang W, Petrovic ZS. Journal of Polymer Science, Part B: Polymer Physics 2004;42(5):809–19.
[18] Petrovic ZS, Zhang W, Zlatanic A, Lava CC, Ilavskyy M. Journal of Polymers and the Environment 2002;10(1/2):5–12.
[19] Petrovic ZS, Guo A, Javni I, Zhang W. Natural fibers, plastics and composites; 2004. p. 167–92.
[20] Petrovic ZS, Cevallos MJ, Javni I, Schaefer DW, Justice R. Journal of Polymer Science, Part B: Polymer Physics 2005;43(22):3178–90.
[21] Javni I, Zhang W, Petrovic ZS. Journal of Applied Polymer Science 2003;88(13): 2912–6.
[22] Javni I, Petrovic ZS, Guo A, Fuller R. Journal of Applied Polymer Science 2000; 77(8):1723–34.
[23] Javni I, Petrovic Z, Zhang W, Guo A. 58th Annual technical conference – society of plastics engineers, vol. 3; 2000. p. 3732–6.
[24] Guo A, Zhang W, Petrovic ZS. Journal of Materials Science 2006;41(15): 4914–20.
[25] Guo A, Javni I, Petrovic Z. Journal of Applied Polymer Science 2000;77(2):467–73.
[26] Sperling LH. Introduction to physical polymer science. 2nd ed. New York, Chichester: Wiley; 1992. p. 1932.
[27] Van Krevelen DW. Properties of polymers: their correlation with chemical structure; their numerical estimation and prediction from additive group contributions. 3rd ed. Amsterdam: Elsevier Science; 1990.
[28] Ryan A. Structure–property relations in poly(urethane–urea)s and polyureas formed by reaction injection moulding, RIM. PhD Thesis, Victoria University of Manchester; 1988.
[29] Rivlin RS, Thomas AG. Journal of Polymer Science 1953;10:291–318.
[30] Lake GJ. Rubber Chemistry and Technology 1995;68(3):435–60.
[31] Russ T, Brenn R, Geoghegan M. Macromolecules 2003;36(1):127–41.
[32] Sommer JU, Russ T, Brenn R, Geoghegan M. Europhysics Letters 2002;57(1): 32–8.
[33] Mark JE. Accounts of Chemical Research 1994;27(9):271–8.
[34] Erman B, Mark JE. Macromolecules 1998;31(9):3099–103.
[35] Sauerbrunn S, Riesen R, Schawe J. Proceedings of the NATAS Annual conference on thermal analysis and applications; 2003; 31st: 013/011–013/018.
[36] Andrady AL, Sefcik MD. Journal of Polymer Science, Polymer Physics Edition 1984.
[37] Mark J, Ngai K, Graessley W, Mandelkern L, Samulski E, Koenig J, et al. Physical properties of polymers. 3rd ed. Cambridge: University Press; 2004.